Erschienen in: IX Brazilian Meeting on Simulational Physics (BMSP 2017) / Vaz da Costa, Bismarck et al. (Hrsg.). - Bristol : IOP Publishing, 2018. - (Journal of Physics : Conference Series ; 1012). - 012011
https://dx.doi.org/10.1088/1742-6596/1012/1/012011

IOP Conf. Series: Journal of Physics: Conf. Series **1012** (2018) 012011 doi:10.1088/1742-6596/1012/1/012011

Brownian Dynamics simulations of model colloids in channel geometries and external fields

Ullrich Siems, Peter Nielaba

Fachbereich Physik, University of Konstanz, 78457 Konstanz, Germany

E-mail: ullrich.siems@uni-konstanz.de

Abstract. We review the results of Brownian Dynamics simulations of colloidal particles in external fields confined in channels. Super-paramagnetic Brownian particles are well suited two-dimensional model systems for a variety of problems on different length scales, ranging from pedestrian walking through a bottleneck to ions passing ion-channels in living cells. In such systems confinement into channels can have a great influence on the diffusion and transport properties. Especially we will discuss the crossover from single file diffusion in a narrow channel to the diffusion in the extended two-dimensional system. Therefore a new algorithm for computing the mean square displacement (MSD) on logarithmic time scales is presented. In a different study interacting colloidal particles were dragged over a washboard potential and are additionally confined in a two-dimensional micro-channel. In this system kink and anti-kink solitons determine the depinning process of the particles from the periodic potential.

1. Introduction

Colloidal particles are a well suited model system [1] to study principle phenomena on all length scales ranging from gravitational collapse [2], over pedestrian walking [3], to two dimensional crystallization [4, 5, 6], glass transition [7] and non-equilibrium phase transition [8]. Besides the use of colloids as model systems the knowledge of their dynamics is crucial for the development of microscopic lab-on-the-chip devices [9] or devices for controlled drug release [10].

This proceeding presents some interesting results of computer simulations of such colloidal model systems. We use Brownian dynamics simulation [11], which is an Euler integration of the overdamped Langevin equation. The positions $\mathbf{r}_i(t)$ of particle i are updated to a new position after the time step Δt

$$\mathbf{r}_i(t+\Delta t) = \mathbf{r}_i(t) + \frac{D_0 \Delta t}{k_B T}\mathbf{F}_i + \sqrt{2D_0\Delta t}\mathbf{R}(t) \ , \tag{1}$$

with microscopic diffusion constant D_0, thermal energy $k_B T$, delta-correlated Gaussian random numbers $\mathbf{R}(t)$ with zero-mean and unit variance, and the deterministic force $\mathbf{F}_i$ acting on this particle. The particles are restricted to the xy-plane, and confined in a channel. Periodic boundary condition is applied in x-direction and hard-wall boundary condition is applied in y-directions. The hard-wall boundary is realized by using the analytically known transition probability of a Brownian particle near a hard boundary as proposed by Behringer and Eichhorn [12]. The length L_X of the channel in x-direction is much larger than the width L_Y in y-directions to avoid finite size effects.

The particles interact via the repulsive potential of parallel dipoles $V = \epsilon(\sigma/r_{ij})^3$, with interaction strength ϵ, particle diameter σ and inter-particle distance $r_{ij} = |\mathbf{r}_i - \mathbf{r}_j|$. This models the interaction of super-paramagnetic colloidal particles in a perpendicular magnetic field, as they were used for experiments in two dimensions [6, 13, 14].
The liquid-solid phase transition in this system is described by the dimensionless control parameter [15]

$$\Gamma = \frac{\epsilon(\sigma)^3}{k_B T R^3} \tag{2}$$

which is given by the ratio of potential energy to thermal energy $k_B T$.

2. Diffusion in channels

In the restricted geometry the particles form layers parallel to the wall [15, 16]. The layering is favored, if the width L_Y of the channel and the spacing R between the layers are commensurable, and otherwise suppressed. In [17] we studied the diffusion in channels with multiple layers of particles at an interaction strength of $\Gamma \approx 12$ near disorder to layer transition. As can be seen from the particle trajectory (Fig. 1 b)) the diffusion strongly depends on the width L_Y of the channel. If layering is favored, the particles diffuse for a long time on their own layer, and only for even longer times they can switch between the layers. If layering is suppressed, the particles can freely diffuse throughout the channel, as in a liquid.
The mean square displacement can be approximated on an intermediate time scale by a power

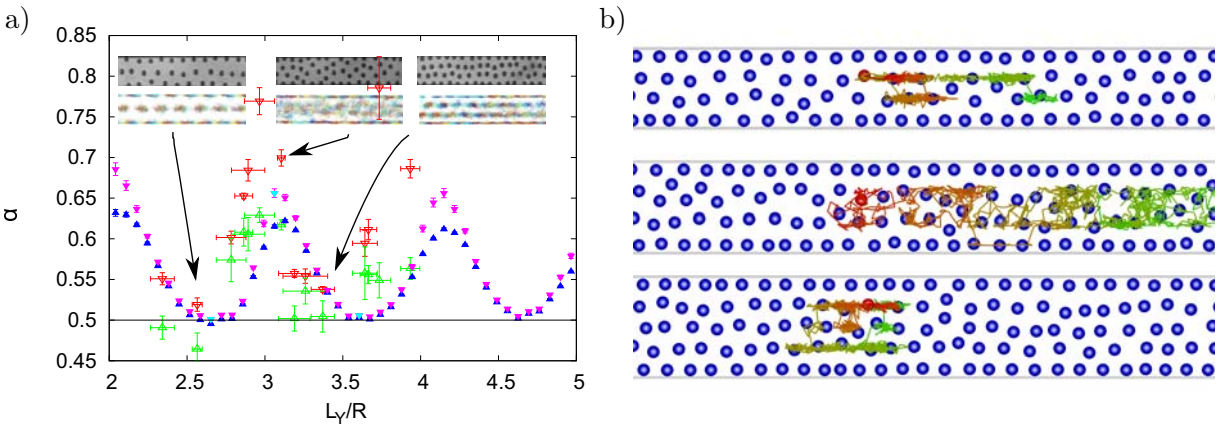

Figure 1. a) Minimal diffusion exponent as a function of reduced channel width L_Y/R, comparing experiments (open symbols with errorbars) and simulation (closed symbols). b) Snapshots of channels of with four layers, five layers and one in between, as well as the trajectory of one particle in each channel with time coloring from green to red. (See Ref. [17])

law $\langle \Delta x^2(t) \rangle \propto t^\alpha$ with exponent α. This exponent is a more universal quantity. For a free particle one finds the normal diffusion exponent $\alpha = 1$ and for particles in a small channel where mutual passing is forbidden one finds the single-file diffusion exponent $\alpha = 0.5$.
This intermediate diffusion exponent is plotted in Figure 1 a) as a function of dimensionless channel width L_Y/R. We see an oscillatory dependency for the simulation results, which is due to the layer structure. If the particles are ordered in layers, the single-file exponent 0.5 can be observed in the intermediate time regime. Otherwise, the MSD is still sub-diffusive in this time regime, but with an exponent greater than the single-file exponent 0.5.

3. Mean Square Displacement

The mean square displacement (MSD) is a quantity that is often used to describe the time dependent self-diffusion of colloidal particles. It measures the averaged squared distance Δx^2 which a particle travels in a time interval Δt. This quantity is averaged over all N particles in the system, and over all possible time origins t_0. Therefore the MSD is calculated by

$$\langle \Delta x^2(\Delta t) \rangle = \frac{1}{N \cdot N_{t_0}} \sum_{t_0} \sum_{i=1}^{N} (x_i\,(t_0 + \Delta t) - x_i(t_0))^2 \ . \tag{3}$$

In a finite simulation of length t_{max} the time differences Δt and the time origins t_0 can be integral multiples of the time step δt and must obey $t_0 + \Delta t \leq t_{max}$. The calculation of the MSD is in this sense of the order of $O(t_{max}^2)$ and therefore becomes the bottleneck of each simulation that normally has a linear time scaling. For this calculation also all positions have to be stored over the total simulation time.

This effort can be reduced drastically: First, because for large time differences Δt the use of each time step as a new time origin t_0 results in an average over multiple dependent time windows. Second, because the MSD is a quantity which varies fast at small Δt and slow at larger Δt. One usually depicts the MSD in a log-log-plot. Hence less sampling points are needed for larger time differences than for smaller ones.

The so called order-n algorithm by Frenkel and Smit [18] solves both of theses problems. But the algorithm is complex, not applicable to other correlation function than the MSD and the sampling points are not evenly spaced on a logarithmic scale. A detailed description of this algorithm is given in the paper of Dubbeldam *et al.* [19]. They also provide an extension of the order-n algorithm to all correlation functions. We present here another method to calculate the MSD much simpler and even a little bit more efficient.

An easier method to reach higher sampling frequencies at small Δt and lower sampling frequencies at large Δt is to directly define the sampling points Δt_n at which the MSD should be calculated. The sampling points should be equally spaced on a logarithmic scale and integral multiples of the time step δt. For simplicity we set the time step $\delta t = 1$. Then the condition for equally spaced integers on a logarithmic scale would be fulfilled for example for sampling points $\Delta t_n = 2^n$ at powers of two. But this would lead to only three points per decade. We choose a power law a^n with a smaller base $2 > a > 1$. For a value of $a = 10^{\frac{1}{15}} \approx 1.166$ we achieve 15 sampling points per decade. To fulfill the condition of integral values we define the time differences

$$\Delta t_n = \mathrm{nint}(a^{n+1-n_{min}} - a^{n_{min}}) \ , \tag{4}$$

with a rounding function nint() and a shift by the constant $n_{min} = \mathrm{nint}\left(1 - \frac{\log(a-1)}{\log(a)}\right)$ which keeps the function injective.

At first glance one could think that it would be sufficient to sample only over non overlapping intervals. Which means to set only every Δt_n a new time origin t_0 for the calculation of $\langle \Delta x^2(\Delta t_n) \rangle$. But this is not true. To achieve a better accuracy than the order-n algorithm one defines a sampling rate

$$R_n = \mathrm{nint}\left(\Delta t_n^b + \frac{1}{2}\right) \ , \tag{5}$$

with constant $b = \left(\frac{\log(30)}{\log(t_{max})}\right)$ for which every R_n time steps a new time origin t_0 is set. The algorithm computes the mean square displacement at the sampling points Δt_n by summing over

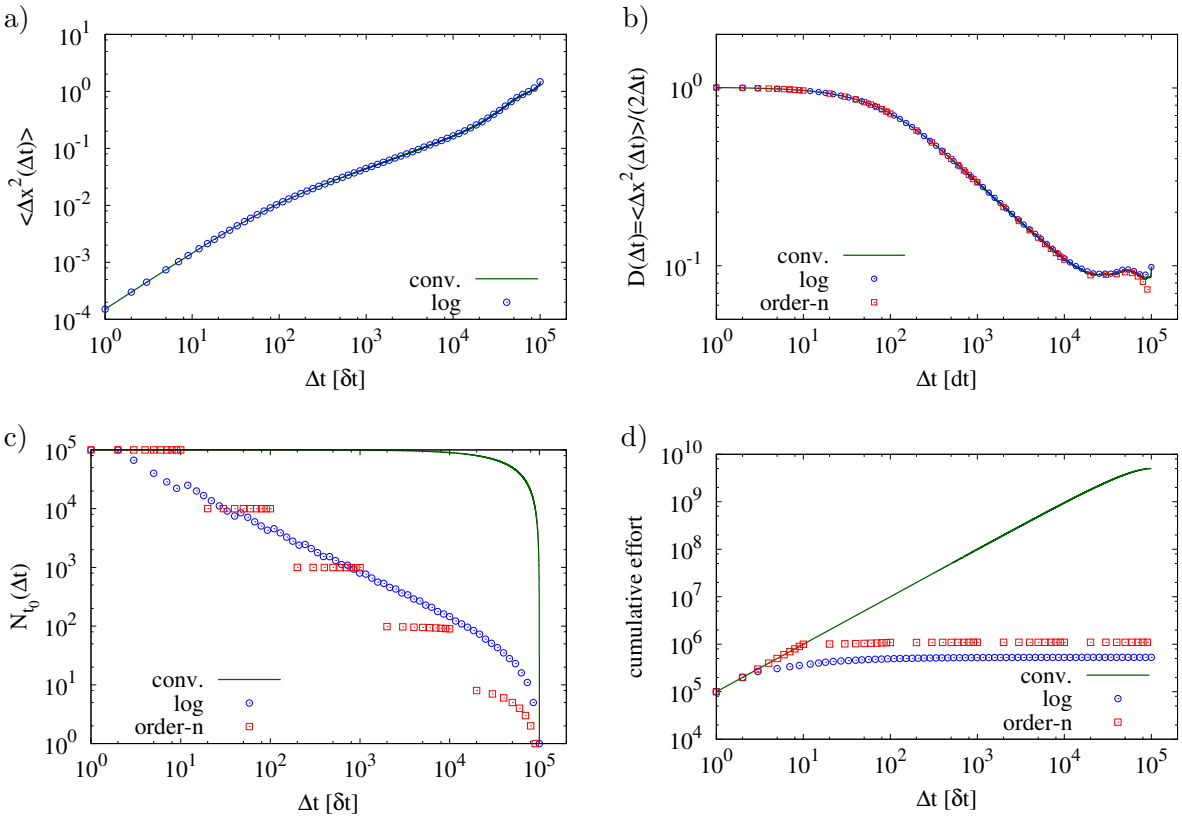

Figure 2. a) The mean square displacement of 300 interacting particles calculated with the log-algorithm (circles) provides comparable accuracy as the MSD calculated with the conventional algorithm (line). b) The time dependent diffusion coefficient shows the deviations of the order-n algorithm (boxes) and the log-algorithm from the results obtained by the conventional algorithm. c) The number of time origins used to calculate the MSD. d) The cumulative effort to calculate the MSD.

all t_0 which are set with different sampling rates R_n.
Figure 2 a) shows the mean square displacement for a simulation of 300 interacting particles with $t_{max} = 10^5$ time steps. The sampling points obtained by the log-algorithm are evenly spaced in the log-log plot, and are close to the curve calculated with the conventional algorithm. In Figure 2 b) a comparison of the time dependent diffusion coefficient $D(\Delta t)$ obtained by the three different methods is given. For the last sampling points the accuracy of the log-algorithm is closer to the conventional algorithm than the order-n algorithm. The reason for this can be seen in Figure 2 c): the log-algorithm uses more time origins than the order-n algorithm for the last few sampling points at large Δt. Since the log-algorithm uses also less time origins for same of the sampling points at small Δt, where the accuracy is already very good, it requires in total less computational time than the order-n algorithm, as can be seen in Figure 2 d).
We provide the algorithm for the MSD calculation within a lattice gas model as test case at https://github.com/ullrichsiems/MSDLOG.

4. Transport in a channel with a periodic potential

In [20] we studied the transport in a channel with a periodic substrate potential along the channel direction and with a constant pulling force acting on each particles along the same direction. We looked at a channel of width $L_Y = 5.2$ with four layers in the "solid" phase at $\Gamma \approx 25$. The external force acting on the particles is

$$\mathbf{F}_{ext} = F\hat{\mathbf{e}}_x + F_C \cos\left(\frac{2\pi}{\lambda}x\right)\hat{\mathbf{e}}_x \ , \tag{6}$$

with a maximal reset force $F_C = 41.8$, different period lengths λ, and a pulling force F which was increased from 0 to 100. This system may be pictured as a wave slide for repelling colloidal particles.

The periodic potential has a strength in the same order of magnitude than the interaction

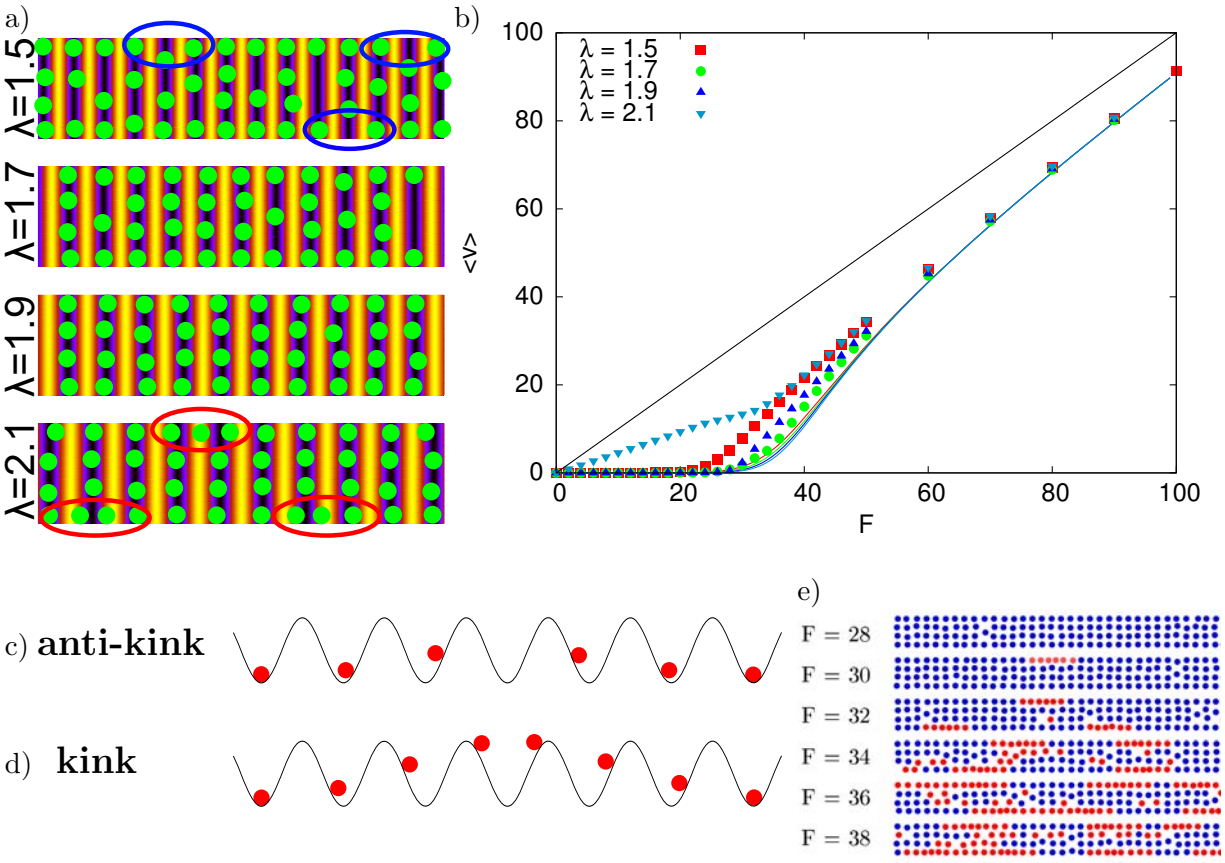

Figure 3. a) Equilibrium particle positions in channels with periodic potentials with different period lengths λ. The potential is color coded with the potential minima in dark. b) Mean particle velocities as a function of the pulling force F for different λ (points) and the solution for a single particle (solid lines). Illustration of c) the kink and d) the antikink soliton of the Frenkel-Kontorova model. e) Snapshot of channel with period length $\lambda = 1.9$ at different pulling forces F, fast particles of moving kinks and anti-kinks are highlighted. (See Ref. [20])

between the particles that enforces the layering parallel to the wall. The potential destroys this layering, and the particles arrange in the minima of the periodic potential (see Fig. 3 a)). Only in the case of $\lambda = 1.9$ the layering with four layers is commensurable with the periodic potential. In this case all minima are occupied by four particles. In the incommensurable cases

there are either vacancies for $\lambda = 1.5$ or additional particles for $\lambda = 2.1$. Both are marked with ellipses (see Fig. 3 a)). The additional particles are located at the boundary layer and they press their neighboring particles a little bit out of the minimum of the periodic potential. This local deformation can be seen as the kink of the Frenkel-Kontorova (FK) model [21] as depicted in Figure 3 d). Whereas the vacancies are the antikinks of the FK model (see Figure 3 c)).
Figure 3 b) shows the mean particle velocities of the particles as a function of the pulling force. In all cases the velocity is increased due to collective effects compared to the solution of a single particle. But in the commensurable case there is no big differences in the mean velocity of the interacting system compared to the single particle picture. For $\lambda = 1.5$ the mean velocity is particularly increased at intermediate forces near the depinning transition, due to the antikinks. The particles can move forward into the vacancy, while the vacancy itself move backwards. For $\lambda = 2.1$ the mean velocity is even more increased. The depinning transition vanishes and the particles already move at low forces, due to the presence of kinks. The extra particles at the boundary can easily be moved, while the attribute of being the extra particles are handed over to the next particle when the particle reaches the next minimum. Therefore the kink excitation moves forwards in the channel faster than the particles themselves. The asymmetry between the kink and antikink can be explained by the purely repulsive interaction. Due to the repulsion kinks can move more easily than antikinks.
How do the particles start to move in the commensurable case with $\lambda = 1.9$, when there is no vacancy a single particle can move into? One could expect that all particles start to move simultaneously at a certain threshold force, but this is not the case. Instead, Figure 3 e) reveals that a particle from one of the mid-layer moves to one of the boundary layer. It leaves an anti-kink on the mid layer and creates a kink on the boundary layer. At the depinning transition, the velocity of the kinks is nearly independent of the external force, but the number of kink and anti-kink pairs increases rapidly. The kink and anti-kinks can pass each other with only a small recombination rate, since they are on different layers. This kind of transport is similar to the conductance in a semiconductor. The kinks at the boundary and anti-kinks on the mid-lane resembles the electrons in the conduction band and holes in the valence band. Although they move in opposite directions, they contribute to a current in the same direction.

5. Diffusion in channels filled with anisotropic particles

As a model for anisotropic particles we used the two-dimensional version of a spherocylinder [22], consisting of a cylinder and two hemispheres rounding off the base and the top of the cylinder. Mathematically a spherocylinder is defined by all points that have the same minimal distance $\sigma/2$ to a line segments of length l, where σ is the diameter of the cylinder base. The aspect ratio of the spherocylinder is $p = (l+\sigma)/\sigma$. The particles interact via the short ranged repulsive Kihara potential [23], which is a function of the minimal distance between the two line segments representing the spherocylinders. The potential has the form of the so called WCA potential which is the repulsive part of the Lennard-Jones potential. The particle-wall interaction is modeled by the same type of interaction.

As an example the results for particles of aspect ratio $p = 2$ are shown. At the beginning of the simulation the particles were organized in four or five layers parallel to the walls, respectively. The width of the channel is varied between $\tilde{L}_Y = 4$ and $\tilde{L}_Y = 5$ at constant particle density. In the early stage of the simulation the particles rearrange according to the width of the channel. When starting with four layers and a width of $\tilde{L}_Y = 4.9$ the particles rearrange in five layers with some skewed particles (see Fig 4 a)). When starting with five layers and a channel width of $\tilde{L}_Y = 4.0$ the spherocylinders rearrange in four layers with some defects (see Fig 4 b)). Even after the rearrangement a orientation along the channel direction dominates. For channels of width $\tilde{L}_Y = 4.5$ the spherocylinders are disordered and orient with a 45 deg angle to the wall. After this quick rearrangement the particles stay in their local cage.

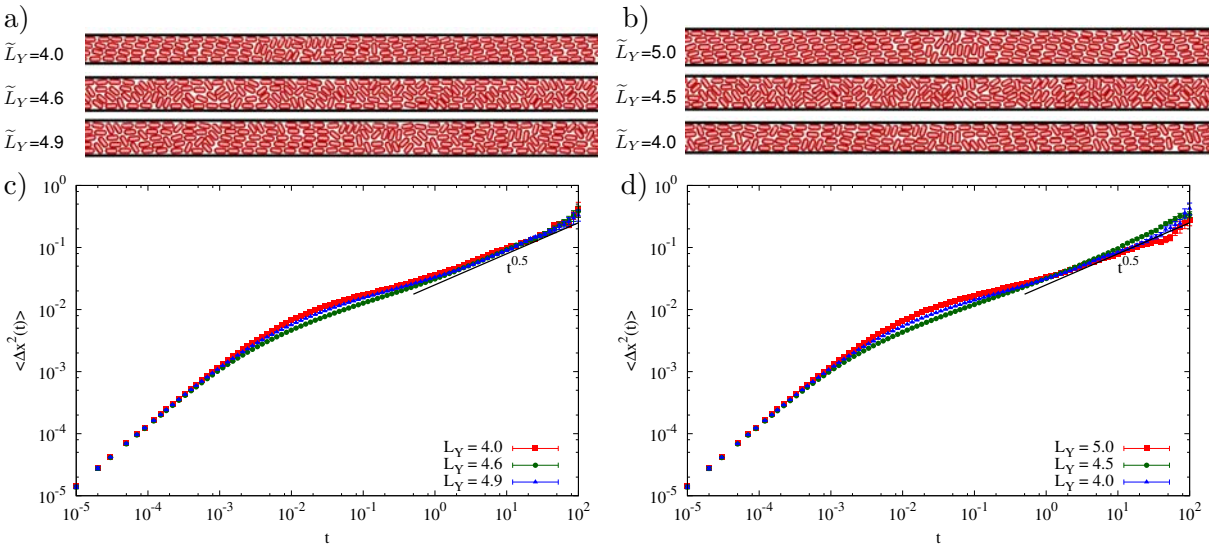

Figure 4. For short spherocylinders with $p = 2$: a) Snapshot after equilibration starting with a configuration of five layers. b) Snapshot after equilibration starting with a configuration of four layers. In c) and d) the mean square displacement along the channel direction is plotted for the above channel systems.

Figure 4 c) and d) show the mean square displacement of the particles along the channel direction after the equilibration phase. In each case the long-time evolution is proportional to $t^{0.5}$, which is a sign of the well known single-file diffusion. Since the system is so dense the particles are locally caged by their neighbors, and only elastic deformations contribute to the mean square displacement. The system can be seen as chain of particles with fixed order, which lead to a single-file diffusion. The intermediate behavior depends on the degree of order and the number of layers in the channel.

Acknowledgments
The authors gratefully acknowledge the SFB 1214 for support and financing the journey to Natal (Brazil), as well as the computing time granted by the John von Neumann Institute for Computing (NIC) and provided on the supercomputer JURECA at Jülich Supercomputing Centre (JSC).

References

[1] Poon W 2004 *Science* **304** 830–831
[2] Bleibel J, Dietrich S, Dominguez A and Oettel M 2011 *Phys. Rev. Lett.* **107** 128302
[3] Helbing D, Farkas I and Vicsek T 2000 *Phys. Rev. Lett.* **84** 1240–1243
[4] Löwen H 1996 *Phys. Rev. E* **53** R29–R32
[5] Zahn K, Méndez-Alcaraz J M and Maret G 1997 *Phys. Rev. Lett.* **79** 175–178
[6] Deutschländer S, Puertas A M, Maret G and Keim P 2014 *Phys. Rev. Lett.* **113** 127801
[7] Illing B, Fritschi S, Kaiser H, Klix C L, Maret G and Keim P 2017 *PNAS* 1856–1861
[8] Heinze B, Siems U and Nielaba P 2015 *Phys. Rev. E* **92** 12323
[9] Squires T and Quake S 2005 *Rev. Mod. Phys.* **77** 977–1026

[10] Yang S Y, Yang J A, Kim E S, Jeon G, Oh E J, Choi K Y, Hahn S K and Kim J K 2010 *ACS Nano* **4** 3817–3822

[11] Ermak D L and McCammon J 1978 *J. Chem. Phys.* **69** 1352–1360

[12] Behringer H and Eichhorn R 2011 *Phys. Rev. E* **83** 065701

[13] Bohlein T, Mikhael J and Bechinger C 2012 *Nat. Mat.* **11** 126–130

[14] Kreuter C, Siems U, Henseler P, Nielaba P, Leiderer P and Erbe A 2012 *J. Phys.: Condens. Matter* **24** 464120

[15] Haghgooie R and Doyle P S 2005 *Phys. Rev. E* **72**(1) 011405

[16] Henseler P, Erbe A, Köppl M, Leiderer P and Nielaba P 2010 *Phys. Rev. E* **81** 041402

[17] Siems U, Kreuter C, Erbe A, Schwierz N, Sengupta S, Leiderer P and Nielaba P 2012 *Scientific Reports* **2** 1015

[18] Frenkel D and Smit B 1996 *Understanding Molecular Simulation* first edition ed (San Diego: Academic Press)

[19] Dubbeldam D, Ford D C, Ellis D E and Snurr R Q 2009 *Molecular Simulation* **35** 1084–1097

[20] Siems U and Nielaba P 2015 *Phys. Rev. E* **91** 022313

[21] Frenkel Y I and Kontorowa T 1938 *Zh. Eksp. Teor. Fiz.* **8** 1340

[22] Löwen H 1994 *Phys. Rev. E* **50** 1232

[23] Kihara T 1953 *Rev. Mod. Phys.* **25** 831–843